International Journal of Innovative
Computing, Information and Control
Volume 11, Number 6, December 2015

ICIC International ©2015 ISSN 1349-4198
pp. 2089–2102

NETWORKED HIERARCHICAL CONTROL SCHEME FOR VOLTAGE UNBALANCE COMPENSATION IN AN ISLANDED MICROGRID WITH MULTIPLE INVERTERS

Lizhen Wu, Xusheng Yang, Xiaohong Hao, Yangyang Lei and Yi Li

School of Electrical and Information Engineering
Lanzhou University of Technology
No. 287, Langongping Road, Lanzhou 730050, P. R. China
wulzh@lut.cn; yangxusheng00@163.com

Received April 2015; revised August 2015

Abstract. *Microgrids (MGs) are deemed as one of the main building blocks of the smart grids. It is important to enhance the power quality in the islanded MGs. However, the power quality can be deteriorated under unbalanced and non-linear loads. In this paper, a Distributed Secondary Control (DSC) method for voltage unbalance compensation in islanded MGs is proposed. Also, based on the communication technology and hierarchical control theory, a new networked hierarchical control scheme is presented for the DSC of MGs. In the control structure, each unit is independently controlled and the entire system of controllers is connected by a communication network. Compared to the centralized secondary control scheme, it makes the MG systems reduce the requirements of communication links bandwidth, toward standardization and be easy to expand. The proposed approach is not only able to compensate voltage unbalance at the Point of Common Coupling (PCC), but also ensures reactive power sharing accurate. The design procedure of the control system is discussed in detail. Finally, simulation experimental results are presented to show the effectiveness of the proposed method in the compensation of voltage unbalance.*

Keywords: Distributed generator (DG), Microgrids (MGs), Networked hierarchical control, Distributed secondary control (DSC), Voltage unbalance compensation

1. **Introduction.** Recently, Microgrids (MGs) have attracted significant attention due to a considerable growth in the number of Distributed Generators (DGs) [1]. MGs are low-voltage distribution networks comprising various Distributed Resources (DRs) and different types of loads and are able to operate either grid-connected or islanded operation modes. DRs may include DGs and distributed storage units [2]. Voltage Source Inverters (VSIs) are usually used for all kinds of distributed generation interfaces in MGs. It is the microgrid's superiority to power the local loads continuously when the utility fails. The voltage and frequency of the MGs are determined by the VSIs in islanded mode; therefore, the compensation of power quality problems can also be achieved through proper control strategies [3]. Amongst various power quality phenomena, voltage unbalances are very common. Voltage unbalance can result in adverse effects on the equipment and power system. Under unbalanced conditions, the power system will incur more losses and be less stable. Also, voltage unbalance has some negative impacts on equipment such as power electronic converters, adjustable speed drives and induction motors. Thus, the International Electro-technical Commission (IEC) recommends the limit of 2% for voltage unbalance in electrical systems [4,5]. A major cause of voltage unbalance is the connection of unbalanced loads (mainly, single-phase loads connection between two phases or between one phase and the neutral).

Compensation of voltage unbalance is usually done using series Active Power Filter (APF) through the injection of negative sequence voltage in series with the distribution line. However, for the microgrid situation, it is uneconomic to install extra APF for each DG [5]. It is well known that DGs often consist of a prime mover that is connected through an interface converter, such as the inverter. Some works have been done on voltage unbalance compensation at the DG terminal through controlling of the Voltage Source Inverters (VSIs). One method for voltage unbalance compensation through the injection of negative-sequence current by the DG has been proposed in [6]. However, under severely unbalanced conditions, the injecting current might be too large. In [7], the unbalanced voltage is compensated with a resonant voltage controller inside the power droop loop and the virtual impedance loop. However, the unbalanced voltage drop on the virtual impedance is not considered, which will lead to unbalance of the output voltage and the compensation effect weakened. In [8], the compensation reference is injected at the output of the voltage control loop. However, such compensation will be considered a disturbance to be rejected by the voltage control loop. Thus, an approach proposed in [9] injects the compensation reference before the voltage controller. A similar control structure is applied in [10], but a Proportional-Integral (PI) controller is used to follow the reference of the voltage unbalance factor. In addition, the droop method has also an inherent trade off between the voltage regulation and the current sharing between the converters [11-15]. In all those techniques, reactive power sharing cannot be achieved completely since voltage is a local variable, as a contrary of frequency. To the end, a hierarchical control concept from the traditional power system has been introduced for MGs in [16,17]. The secondary control has been proposed to restore the nominal values of the voltage inside the MGs.

To solve the problem and accomplish the voltage harmonics compensation simultaneously, in this paper, the Distributed Secondary Control (DSC) strategy is applied to compensate the voltage unbalance at PCC for an islanded MG. Also a simple networked hierarchical control scheme is presented for the DSC of MGs, which avoids the use of a single centralized controller for the secondary level of MGs. In this control architecture, the primary and secondary controllers are implemented together locally in each DG, where the secondary control should collect the required data from all other units and produce appropriate reference control signal. This way, every DG has its own local secondary control that can produce appropriate control signal for the primary control level by using the measurements of other DGs in each sample time.

The paper is organized as follows. Section 2 discusses the structure of the microgrid hierarchical control. The design approach of the control system is presented in Section 3, including DG local control strategy and distributed secondary control strategy. Section 4 includes simulation experimental results. Finally, the paper is concluded in Section 5.

2. Networked Hierarchical Control Structure of Microgrid.

Hierarchical control applied to power dispatching in power systems is well known, and it has been used extensively for decades. Nowadays, these concepts are starting to be applied to MGs based on power-electronic, which are able to operate both in grid-connected and in island mode. The hierarchical control approach makes the MGs toward standardization, smartness and flexibility. A hierarchical control structure consisting of three control levels is proposed in [16-19]. The primary control deals with the local control of the DG units, which is based on the droop method including a virtual output-impedance loop. The secondary level is designed to restore the DGs output voltage frequency and amplitude deviations, which are produced by the power droop-controllers and output impedances. The tertiary control

level exchanges information with the distribution system operator in order to make feasible and to optimize the MG operation within the utility grid [19]. Moreover, primary and tertiary controls are decentralized and centralized control levels respectively, since while one is taking care of the DG units, the other concerns about the MG global optimization. Since, in this paper, the microgrid operates in islanded mode, the tertiary control level is not considered. Secondary control is conceived to compensate frequency and voltage deviations produced inside the MG by the virtual inertias and output virtual impedances of primary control [20,21]. However, the conventional secondary control approach depends on using a MicroGrid Central Controller (MGCC), which includes slow controls loops and low bandwidth communication systems in order to measure some parameters in certain points of the MG, and to send back the control output information to each DG unit. The drawback is that the MGCC is not highly reliable since a failure of this controller is enough to stop the secondary control action. Moreover, the centralized control strategy has an inherent drawback of the single point of failure, i.e., an MGCC failure terminates the secondary control action for all units.

The problem of using the MGCC for implementing secondary control is that a failure can result in a bad function of the whole system. In order to avoid a single centralized controller, a networked hierarchical control scheme is presented for the DSC of MGs in this paper. A distributed control strategy is an approach in which none of the controllers are centralized, but distributed throughout the system so that each unit is independently controlled and the entire system of controllers is connected by a communication network. The main idea is to implement primary and secondary controllers together as a local controller. In this sense, a local secondary control is determined for each DG to generate set-points of the droop control to restore the deviations produced by the primary control. This kind of distributed control strategies, also named Networked Control Systems (NCS), has been reported recently in some literature [22,23]. However, in [22], technical aspects of providing frequency control reserves (FCRs) and the potential economic profitability of participating in FCR markets for both decentralized and centralized coordination approach based on a setup of multiple MGs are investigated. On the other hand, a master-slave control by using networked control strategy for the parallel operation of inverters has been introduced in [23]. The method is employed to achieve the superior load-sharing accuracy compared to conventional droop scheme. However, the application of these control strategies to secondary control of MGs still has not been proposed. So, in this work, a networked hierarchical control scheme is presented for the secondary control of MGs.

Figure 1 shows the diagram of a general architecture of networked hierarchical control for islanded MGs. In this architecture, primary and secondary controls are implemented in each DG unit. The secondary control is placed between the communication system and the primary control. In other word, the secondary control is locally embedded in each DG unit, similar to primary control; however, the local secondary control requires an underlying communication network to operate properly. Since the secondary control should collect the required data from all other units and produce appropriate control signal for the primary one using an averaging method. In turn, the local secondary controllers operate on these parameters, and proposed communication algorithm is able to not only control frequency and voltage but also share power between units in the MG. Data exchange for DSC can be implemented in industrial Ethernet or EtherCAT.

3. **The Control System Design for Voltage Unbalance Compensation.**

In the primary control level, voltage, current, and virtual impedance control loops are designed without considering the effect of unbalance compensation; then, in the secondary control

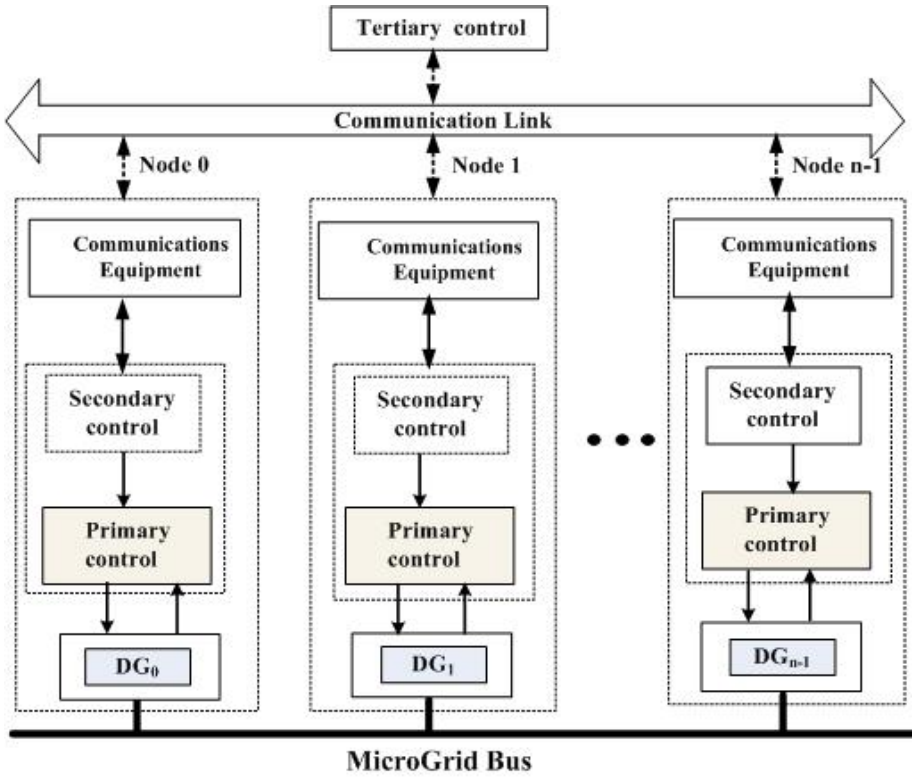

FIGURE 1. General architecture of networked hierarchical control for islanded MGs

level, compensation gain is selected such that the stability of the compensated system is ensured. Frequency control, voltage control, and reactive power sharing will also be reviewed by using this control approach. The present paper mainly focuses on the voltage quality at PCC.

The proposed networked hierarchical control structure and the DG power stage are shown in Figure 2. It can be seen that the power stage of each DG consists of a DC power, an interface inverter and an LC filter. The impedance Z_{l1} models the distribution line between DG_1 and PCC. Note that, the other DGs have the same power stage, but the line impedances are different. The local controller of each DG consists of voltage and current control loops, virtual impedance loop, and active/reactive power droop controllers, which generate the gate signals for DGs interface inverters. The secondary controller generates the unbalance compensation of PCC voltage in microgrid by sending proper control signals to the DGs local controllers. Then, in order to extract PCC voltage positive and negative sequences, which are transmitted toward the secondary controller to calculate Voltage Unbalance Factor (VUF). More details about the design of the primary and secondary controllers are provided in the next section.

3.1. **The design of DG inverter local control level.** The DG local control system is shown in Figure 2. At first, DG three-phase output voltage and current (v_{oabc} and i_{oabc}, respectively) are measured and transformed to $\alpha\beta$ frame. Secondly, positive and negative sequences of output voltage and positive sequence of output current are extracted. Positive sequence current is fed to the virtual impedance block. Then, the voltage controller follows the references generated by power controllers and secondary controllers to generate the reference for the current controller. Moreover, the power controllers are designed by the active and reactive droop control method, whose outputs E^* and ϕ^* are used to generate the three phase reference voltages of the inverter. This voltage is positive

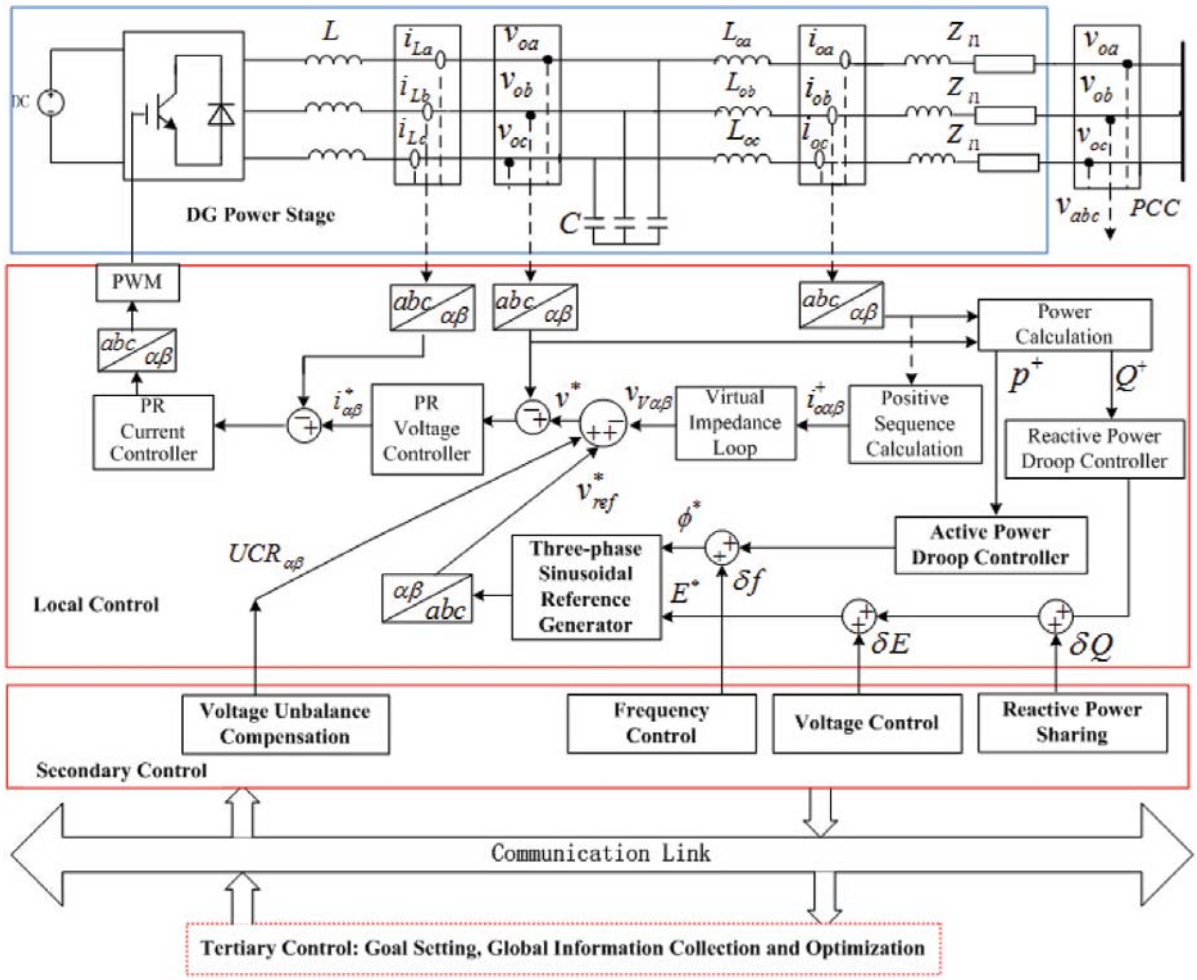

FIGURE 2. Scheme of the proposed networked hierarchical control for a DG unit in MG

sequence component; thus, positive sequence powers must be calculated before. The output of the current controller is transformed back to *abc* frame to provide three-phase voltage reference for the Pulse Width Modulator (PWM). Finally, the PWM block controls the switching of the inverter based on this reference. More details are provided in the following subsections.

As shown in Figure 2, the DG local control system is designed in $\alpha\beta$ reference frame. So, the clarke transformation is used to transform the variables between *abc* and $\alpha\beta$ frames. The transformations are shown in Equations (1) and (2).

$$\begin{pmatrix} x_\alpha \\ x_\beta \end{pmatrix} = \sqrt{\frac{2}{3}} \begin{pmatrix} 1 & -\frac{1}{2} & -\frac{1}{2} \\ 0 & \frac{\sqrt{3}}{2} & -\frac{\sqrt{3}}{2} \end{pmatrix} \cdot \begin{pmatrix} x_a \\ x_b \\ x_c \end{pmatrix} \tag{1}$$

$$\begin{pmatrix} x_a \\ x_b \\ x_c \end{pmatrix} = \sqrt{\frac{2}{3}} \begin{pmatrix} 1 & 0 \\ -\frac{1}{2} & \frac{\sqrt{3}}{2} \\ -\frac{1}{2} & -\frac{\sqrt{3}}{2} \end{pmatrix} \cdot \begin{pmatrix} x_\alpha \\ x_\beta \end{pmatrix} \tag{2}$$

where x_a, x_b, x_c and x_α, x_β can represent the instantaneous output voltage (v_{oa}, v_{ob}, v_{oc} and $v_{o\alpha}$, $v_{o\beta}$), output current (i_{oa}, i_{ob}, i_{oc} and $i_{o\alpha}$, $i_{o\beta}$), or LC filter inductor current (i_{La}, i_{Lb}, i_{Lc} and $i_{L\alpha}$, $i_{L\beta}$) in the *abc* and $\alpha\beta$ frames, respectively.

3.1.1. *The design of the improved droop controllers.* The conventional frequency/voltage droop method is a well studied strategy; however, it has important drawbacks. Although it is useful to share a common active load between DGs, the reactive power control scheme is strongly dependent on the grid parameters. The power-sharing accuracy is strongly affected by impedance unbalances [24]. The imminent frequency and magnitude deviations can strongly affect the system stability. High droop gains have a negative impact on the stability of the system. It is not suitable when nonlinear load is shared [25]. So this paper proposed an approach to overcome these problems and provide improved solutions to the control of stand-alone mode microgrids.

Considering a three-phase DG that is connected to the grid through the impedance $Z\angle\theta$, the fundamental positive sequence active and reactive powers injected to the grid by the DG (P^+ and Q^+, respectively) can be expressed as follows [20]:

$$P^+ = \left(\frac{EV}{Z}\cos\phi - \frac{V^2}{Z}\right)\cos\theta + \frac{EV}{Z}\sin\phi\sin\theta \tag{3}$$

$$Q^+ = \left(\frac{EV}{Z}\cos\phi - \frac{V^2}{Z}\right)\sin\theta - \frac{EV}{Z}\sin\phi\cos\theta \tag{4}$$

where P^+ and Q^+ are the positive sequence active power and positive sequence reactive power, respectively. E is the magnitude of the inverter output voltage, V is the grid voltage magnitude, ϕ is the load angle between E and V, and Z and θ are the magnitude and the phase angle of the impedance, respectively. Considering phase angle of the grid voltage to be zero, ϕ will be equal to phase angle of the inverter voltage. Assuming mainly inductive electrical systems ($Z \approx X$ and $\theta \approx 90°$), the active and reactive powers can be expressed as the following equations:

$$P^+ = \frac{EV}{X}\sin\phi \tag{5}$$

$$Q^+ = \frac{EV\cos\phi - V^2}{X} \tag{6}$$

In practical applications, ϕ is normally small; thus, a P^+ and Q^+ decoupling approximation ($\cos\phi \approx 1$ and $\sin\phi \approx \phi$) can be considered as follows [20]:

$$P^+ \approx \frac{EV}{X}\phi \tag{7}$$

$$Q^+ \approx \frac{V(E-V)}{X} \tag{8}$$

Thus, active and reactive powers can be controlled by the DG output voltage phase angle and amplitude, respectively. According to this, the following droop controller is designed for the positive sequence active and reactive power sharing among DGs in an islanded microgrid:

$$\phi^* = \frac{\omega^*}{s} = \frac{1}{s}\left[\omega_0 - (m_p + m_D s)P^+\right] \tag{9}$$

$$E^* = E_0 - n_p Q^+ \tag{10}$$

where, s is the Laplace variable; E_0 is the rated voltage amplitude; ω_0 is the rated angular frequency; m_p is the active power proportional coefficient; m_D is the active power integral coefficient; n_p is reactive power proportional coefficient; E_0 is voltage amplitude reference; ϕ^* is voltage phase angle reference ($\phi^* = \int \omega^* dt$).

If the microgrid operates in islanded mode, the use of pure integrators is not allowed, since, the total load will not coincide with the total injected power, and it will lead to instability [25]. So the traditional droop control method must be improved. In this paper,

no integral term is considered for voltage frequency and amplitude control. Moreover, the derivative coefficient in Equation (9), m_D helps to improve the dynamic behavior of the power control.

According to the instantaneous reactive power theory [26,27], the instantaneous values of active and reactive powers should be calculated using (11) and (12), respectively:

$$p = \nu_{o\alpha} i_{o\alpha} + \nu_{o\beta} i_{o\beta} \tag{11}$$

$$q = \nu_{o\beta} i_{o\alpha} - \nu_{o\alpha} i_{o\beta} \tag{12}$$

Each of the instantaneous powers consists of *dc* and *ac* (oscillatory) components. The *dc* components (average values of p and q) are positive sequence active and reactive powers (P^+ and Q^+, respectively) [27]. The oscillatory parts are generated by the unbalance and/or harmonic contents of the voltage and current. The *dc* components are extracted using two 1st order low pass filters in the following.

$$LPF(s) = \frac{\omega_c}{s + \omega_c} \tag{13}$$

where s represents the Laplace variable, and $LPF(s)$ is the transfer function of Low Pass Filter (LPF), i.e., the cut-off frequency of these filters is set to 4π (rad/s).

3.1.2. *The design of the virtual impedance loop.* The accuracy of the power sharing provided by the droop controllers is affected by the output impedance of the DG units and the line impedances. The virtual impedance is a fast control loop that can fix the phase and magnitude of the output impedance. Moreover, the effect of asymmetrical line impedances can be mitigated by proper design of the virtual impedance loop [20,21]. In contrast with physical resistance, the virtual resistance has no power losses, because it is provided by a control loop; thus, it is possible to implement it without decreasing the efficiency [20]. In addition, virtual inductance is considered to make the DG output impedance more inductive to improve the decoupling of P^+ and Q^+. Thus, the virtual impedance enhances the performance and stability of droop controllers. Furthermore, the virtual output impedance can provide additional features such as the hot-swap operation and sharing of nonlinear load.

The virtual impedance is implemented as shown in Figure 3, where R_ν and L_ν are the virtual resistance and inductance values, respectively [28]. Thus, the following equations express the virtual impedance in the $\alpha\beta$ frame:

$$\nu_{V\alpha} = R_\nu i^+_{o\alpha} - L_\nu \omega i^+_{o\beta} \tag{14}$$

$$\nu_{V\beta} = R_\nu i^+_{o\beta} + L_\nu \omega i^+_{o\alpha} \tag{15}$$

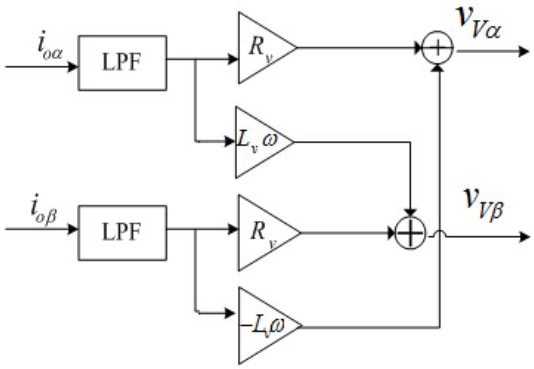

FIGURE 3. The block diagram of virtual impedance

3.1.3. *The design of the proportional-resonant voltage and current controllers.* Due to the difficulties of using Proportional-Integral (PI) controllers to track non-dc variables, quasi Proportional-Resonant (PR) controllers are usually preferred to control the voltage and current in a stationary reference frame [20,29]. In this paper, the following quasi PR voltage and current controllers are applied.

$$G_V(s) = k_{pV} + \sum_{k=1,3,5,7} \frac{2k_{rV} \cdot \omega_{cV} \cdot s}{s^2 + 2\omega_{cV} \cdot s + (k\omega_0)^2} \tag{16}$$

$$G_I(s) = k_{pI} + \sum_{k=1,3,5,7} \frac{2k_{rI} \cdot \omega_{cI} \cdot s}{s^2 + 2\omega_{cI} \cdot s + (k\omega_0)^2} \tag{17}$$

where k_{pV} (k_{pI}) and k_{rV} (k_{rI}) are the proportional and kth harmonic resonant coefficients of the voltage (current) controller, respectively. Also, ω_{cV} and ω_{cI} represent the voltage and current controller cut-off frequencies, respectively.

3.2. **The design of the secondary control level.** It is well known that voltage unbalance leads to the appearance of the negative-sequence voltage. Thus, the compensation of voltage unbalance can be achieved by reducing the negative-sequence voltage. As shown in Figure 2, the output of the Unbalance Compensation Reference (UCR) is injected as a reference for the voltage controller. The details of this calculation are shown in Figure 4.

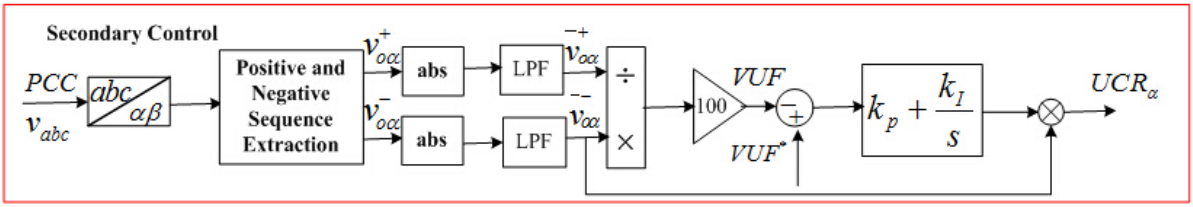

FIGURE 4. Block diagram of secondary control level

According to Figure 4, at first the three-phase output voltage of PCC is measured and transformed to the $\alpha\beta$ frame ($v_{o\alpha\beta}$). Secondly, positive and negative sequences of output voltage of PCC ($\nu^+_{o\alpha}$ and $\nu^-_{o\alpha}$) are extracted, which are used to calculate Voltage Unbalance Factor (VUF) [20]. As can be seen, α-components of PCC output voltage positive and negative sequences are fed to VUF calculation block. Then, the average values of rectified waveforms ($\overline{\nu}^+_{o\alpha}$ and $\overline{\nu}^-_{o\alpha}$) are calculated by applying two absolute functions (abs) and Low-Pass Filters (LPF). LPF structure and parameters are exactly as follows.

$$LPF = \frac{\omega_{cut}^2}{s^2 + 2\zeta\omega_{cut}s + \omega_{cut}^2} \tag{18}$$

where, the filter cut-off frequency $\omega_{cut} = 4\pi$ (rad/s) and the damping ratio $\zeta = 0.707$.

Afterwards, the calculated value is compared with the reference VUF^* and the error is fed to a PI controller. Finally, the output of PI controller is multiplied by $\overline{\nu}^-_{o\alpha}$ to generate UCR_α, which is transmitted to the primary level. It is noteworthy that the β-components are used for VUF calculation, the result will be the same, because the positive and negative sequences are balanced.

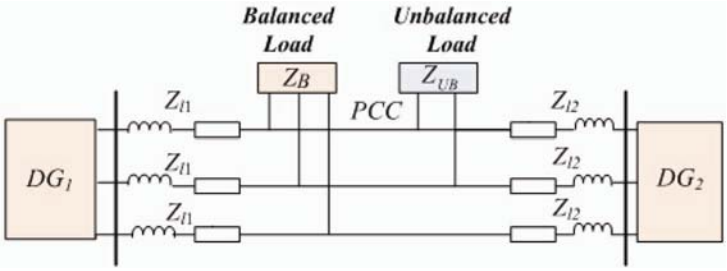

FIGURE 5. Test system of simulation studies

4. **Simulation Experiment Results Analysis.** The simulation experiments are performed using the MATLAB/Simulink software package and the Control Desk with a TMS320F2812 DSP controller card. The simulation experiments of voltage unbalance compensation considering Resistive-Inductive (RI) and resistive loads are presented. Several simulation experimental tests including the comparison with extant technique were carried out to validate the effectiveness of the proposed scheme.

The islanded microgrid shown in Figure 5 is considered the test system for simulation studies and also the experimental evaluation of voltage unbalance compensation.

TABLE 1. Power stage parameters

DG prime mover	Inverter filter inductance	Inverter filter capacitance	DG1 distribution line	DG2 distribution line	Unbalanced load	Balanced load
V_{dc} (V)	L (mH)	C (μF)	Z_{l1} (Ω)	Z_{l2} (Ω)	Z_{UB} (Ω)	Z_a (Ω)
650	1.8	25	$0.6 + j1.6959$	$0.2 + j0.5655$	660	$50 + j12.57$

TABLE 2. Control system parameters

Primary Level													Secondary Level	
Power Controllers					Virtual Impedance		Voltage Controller			Current Controller			PI Controller	
m_D	m_p	n_p	E_0	ω_0	R_ν (Ω)	L_ν (mH)	k_{pV}	k_{rV}	ω_{cV}	k_{pI}	k_{rI}	ω_{cI}	k_p	k_I
0.00002	0.0002	0.13	$230\sqrt{2}$	$2\pi * 50$	1	4	2	100	2	10	1000	2	0.5	7

This microgrid includes two DGs with the power stage and control system, as shown in Figure 2. It can be seen from Figure 5, a single-phase load Z_{UB} is connected between phases "a" and "b" which creates voltage unbalance. A balanced star-connected three-phase load Z_B is also connected to PCC. Power stage and control system parameters are listed in Tables 1 and 2, respectively. To provide correct comparison, the power stage and control system parameters remain consistent with the extant techniques proposed in [21]. Switching frequency of the DGs inverters is set to 10 kHz. In this figure, Z_{l1} and Z_{l2} represent the distribution lines between DGs and PCC. Unbalance compensation starts acting from $t = 0.5$s. VUF^* is set to 0.5%.

As shown in Figure 6(a), VUF of PCC properly follows the reference value. Also, it can be seen that the improvement of PCC voltage quality is achieved by making the DGs output voltage unbalanced. Also, its VUF is increased a little more because of the less line impedance between DG_2 and the PCC. The simulation result of the conventional secondary control approach proposed in [21] was shown in Figure 6(b). It can be seen that the VUF of PCC also can follow the reference value, but VUF of DGs increases more than Figure 6(a). It will make the voltage unbalance of DGs increase, even over the limit. By comparing the result, it can illustrate that the proposed approach has better compensation results.

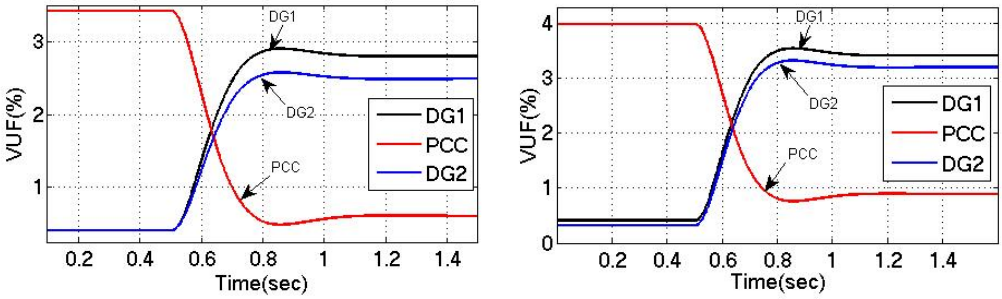

(a) The VUF of the proposed approach (b) The VUF of the proposed approach in [21]

FIGURE 6. VUF at PCC and DGs terminal

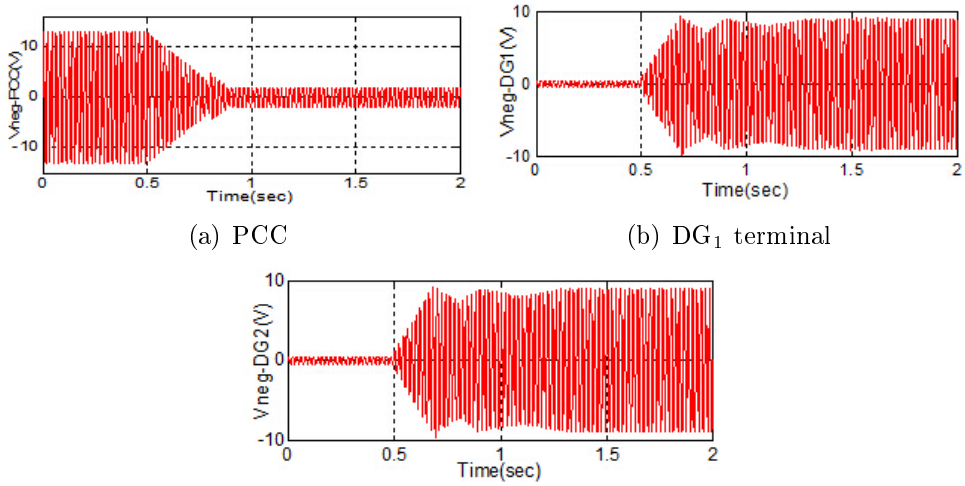

(a) PCC (b) DG_1 terminal

(c) DG_2 terminal

FIGURE 7. Phase-a negative sequence voltages

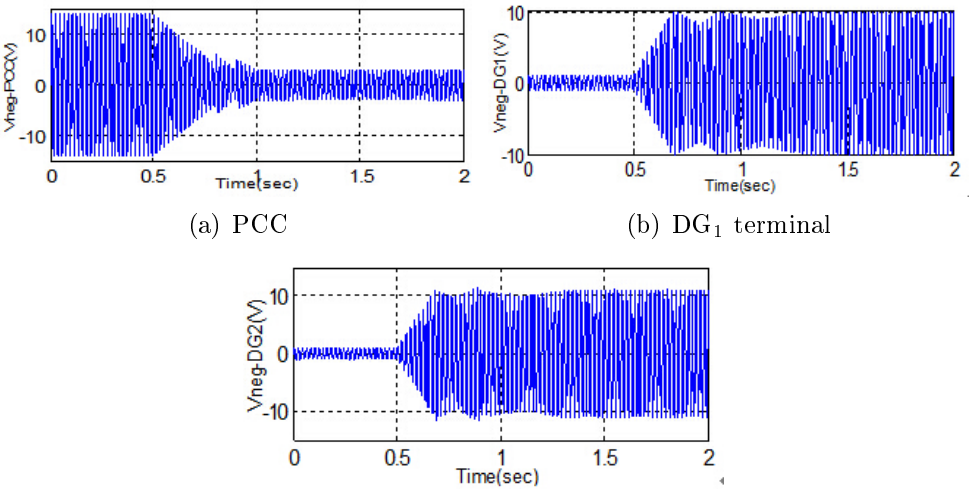

(a) PCC (b) DG_1 terminal

(c) DG_2 terminal

FIGURE 8. Phase-a negative sequence voltages in [21]

To provide more details, the simulation results of phase-a negative sequence voltage at PCC and DGs terminal are shown in Figures 7(a)-7(c). As seen, PCC negative sequence voltage is decreased by increase of DGs output voltage negative sequence. The result proposed in [21] was shown in Figures 8(a)-8(c). It can be seen from Figures 8(a)-8(c) that the negative sequence voltage is slightly higher and the fundamental negative sequence component cannot be shared properly. By comparing the results, it can be concluded that the proposed approach can compensate the voltage unbalance at PCC of MGs, which proves that the proposed approach has practical value.

In addition, compared to the control structure, the problem in [21] is using the MGCC to implement secondary control that will result in low reliability and heavy communication burden. This work using DSC strategy overcomes the inherent drawback of using centralized control strategy. The control strategy proposed in this paper not only enhances the power quality, but also reduces the requirement of communication link bandwidth. Moreover, it can make the MGs toward smartness, standardization, flexibility, and be easy to expand. It makes the MGs easy to implement plug and play functions.

Also, in order to demonstrate unbalance compensation more clearly, the before compensation and after compensation waveforms of three-phase output voltages at PCC and DG_1 terminal are depicted in Figure 9. The DG_2 output voltage behavior is similar to DG_1. As seen, as a result of compensation, PCC voltage unbalance is decreased, effectively; while the DG_1 output voltage becomes unbalanced. These figures demonstrate the effectiveness of the proposed compensation method in balancing the PCC output voltages.

The simulation and experimental results of before compensation and after compensation waveforms at PCC three-phase output currents are depicted in Figure 10. Because

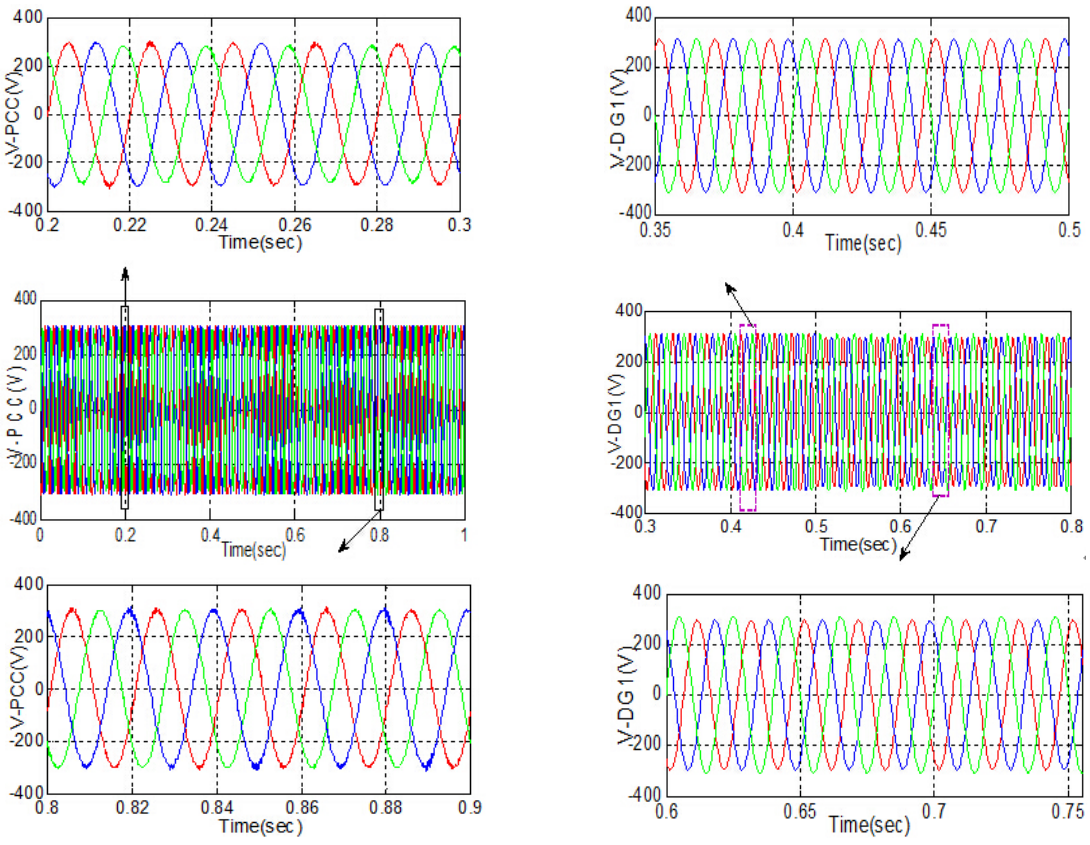

(a) PCC (b) DG_1 terminal

FIGURE 9. Three-phase voltages. (a) PCC. (b) DG_1 terminal.

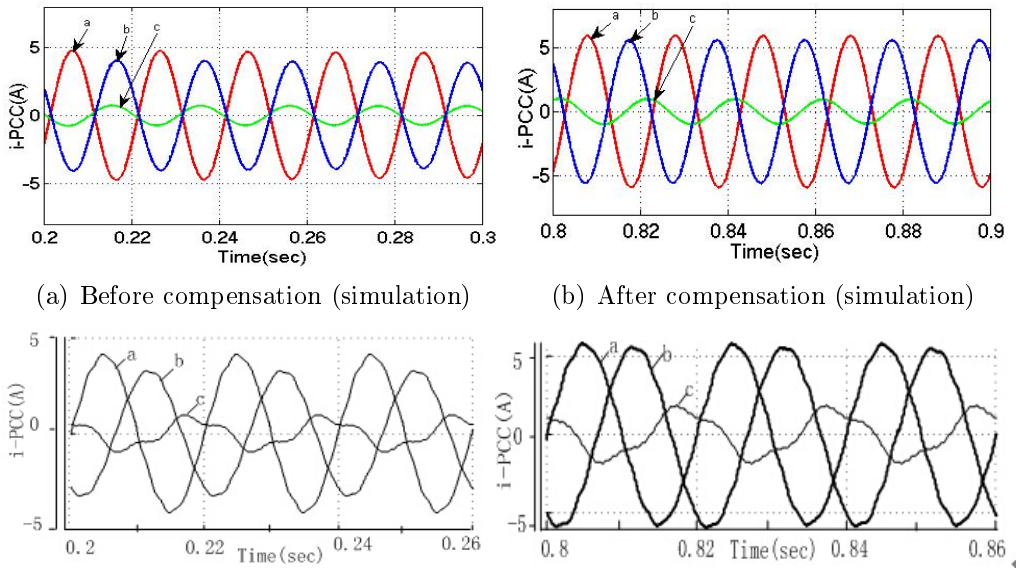

(a) Before compensation (simulation) (b) After compensation (simulation)

(c) Before compensation (experimental) (d) After compensation (experimental)

FIGURE 10. PCC output current

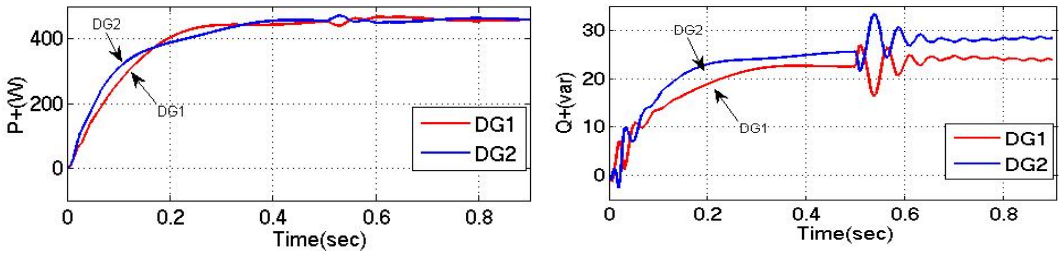

(a) Active power (b) Reactive power

FIGURE 11. Power sharing

the load is connected between phase-a and phase-b, the currents of these phases are approximately the same (red and blue waveforms, respectively), and the phase-c current (green waveform) is approximately zero. The unbalance load currents create voltage unbalance; thus, the compensation control loop action leads to a slight increase of the phase-c current to reduce voltage unbalance. These results show the effectiveness of the voltage unbalance compensation. In addition, the experimental and simulation results are in good agreement.

Sharing of P^+ and Q^+ between DGs are shown in Figures 11(a) and 11(b) respectively. As seen, in spite of asymmetrical distribution lines, active and reactive powers are shared properly between the DGs. Also, it should be noted that the active power can be shared exactly between DGs, because the frequency is the same throughout the microgrid, while, due to no uniform profile of microgrid voltage, reactive power is shared by a small error.

5. **Conclusions.** In this paper, a networked hierarchical control approach for PCC voltage unbalance compensation in an islanded microgrid is proposed. The control structure consists of DGs local controllers and a distributed secondary controller. In this architecture, the primary and secondary controllers are implemented together locally in each DG, where the secondary controller collects the required data from all other units and

produces appropriate control signal for the primary one using an averaging method. Data exchange for DSC can be implemented in communication networks, such as industrial Ethernet or EtherCAT. However, every secondary controller calculates PCC voltage unbalance compensation and directly sends the proper control signals to the local controllers in the primary level by interline. PCC voltage data and the control signal are transmitted to/from secondary level through interline. The distributed secondary control does not rely on a central control, so that the failure of a single unit will not produce the fail down of the whole system. The design of control system is discussed. The simulation experimental results show that the PCC voltage unbalance is compensated to the desired value, while active and reactive powers are shared properly.

As the next step, a non-linear load should be considered. Since this paper only presented and compared the results of voltage unbalance compensation considering resistive and resistive-inductive loads. We are working on the secondary control for compensation of the other PCC voltage power quality problems such as voltage harmonics and sags. In addition, this paper neglects delays and packet losses, so the time delay limits of the communication systems will be studied as well.

Acknowledgment. This work was supported by the National Natural Science Foundation of China (No. 51467009), Science and Technology Foundation of STATE GRID Corporation of China, the project of Lanzhou science and technology plan (No. 2014-1-162).

REFERENCES

[1] J. M. Guerrero, F. Blaabjerg, T. Zhelev et al., Distributed generation: Toward a new energy paradigm, *IEEE Ind. Electron. Mag.*, vol.4, no.1, pp.52-64, 2010.

[2] C. A. Canizares and R. Palma-Behnke, Trends in microgrid control, *IEEE Trans. Smart Grid*, vol.5, no.4, pp.1905-1918, 2014.

[3] R. Majumder, Some aspects of stability in microgrids, *IEEE Trans. Power Systems*, vol.28, no.3, pp.3243-3252, 2013.

[4] A. V. Jouanne and B. Banerjee, Assessment of voltage unbalance, *IEEE Trans. Power Del.*, vol.16, no.4, pp.782-790, 2001.

[5] M. Hamad, M. Masoud and B. Wayne Williams, Medium-voltage 12-pulse converter: Output voltage harmonic compensation using a series APF, *IEEE Trans. Ind. Electron.*, vol.61, no.1, pp.43-52, 2014.

[6] M. Hamzeh, H. Karimi and H. Mokhtari, Harmonic and negative-sequence current control in an islanded multi-bus MV microgrid, *Trans. Smart Grid*, vol.5, no.1, pp.167-176, 2014.

[7] P. T. Cheng, C. Chen, T. L. Lee and S. Y. Kuo, A cooperative imbalance compensation method for distributed-generation interface converters, *IEEE Trans. Ind. Appl.*, vol.45, no.2, pp.805-815, 2009.

[8] M. Savaghebi, J. M. Guerrero, A. Jalilian and J. C. Vasquez, Experimental evaluation of voltage unbalance compensation in an islanded microgrid, *IEEE Trans. Ind. Electron.*, vol.58, no.3, pp.1453-1458, 2011.

[9] M. Datta, T. Senjyu, A. Yona, T. Funabashi and K. Chul-Hwan, A coordinated control method for leveling PV output power fluctuations of PV-diesel hybrid systems connected to isolated power utility, *IEEE Trans. Energy Convers*, vol.24, no.1, pp.153-162, 2009.

[10] D. E. Olivares, C. A. Canizares and M. Kazerani, A centralized energy management system for isolated microgrids, *IEEE Trans. Smart Grid*, vol.5, no.4, pp.1864-1875, 2014.

[11] B. Singh and J. Solanki, An implementation of an adaptive control algorithm for a three-phase shunt active filter, *IEEE Trans. Ind. Electron.*, vol.56, no.8, pp.2811-2820, 2009.

[12] J. C. Vasquez, R. A. Mastromauro, J. M. Guerrero and M. Liserre, Voltage support provided by a droop-controlled multifunctional inverter, *IEEE Trans. Ind. Electron.*, vol.56, no.11, pp.4510-4519, 2009.

[13] K. Borisov and H. L. Ginn, Multifunctional VSC based on a novel Fortescue reference signal generator, *IEEE Trans. Ind. Electron.*, vol.57, no.3, pp.1002-1007, 2010.

[14] J. Dannehl, M. Liserre and F. W. Fuchs, Filter-based active damping of voltage source converters with LCL filter, *IEEE Trans. Ind. Electron.*, vol.58, no.8, pp.3623-3633, 2011.

[15] J. M. Guerrero, J. C. Vasquez, J. M. Alcala, L. G. de Vicuna and M. Castilla, Hierarchical control of droop-controlled AC and DC microgrids – A general approach toward standardization, *IEEE Trans. Ind. Electron.*, vol.58, no.1, pp.158-172, 2011.

[16] A. Bidram and A. Davoudi, Hierarchical structure of microgrids control system, *IEEE Trans. Smart Grid*, vol.3, no.4, pp.1963-1976, 2012.

[17] A. Bidram, A. Davoudi, F. L. Lewis and Z. Qu, Secondary control of microgrids based on distributed cooperative control of multi-agent systems, *IET Gener. Transm. Distrib*, vol.7, no.8, pp.822-831, 2013.

[18] L. Meng, F. Tang, M. Savaghebi, J. C. Vasquez and J. M. Guerrero, Tertiary control of voltage unbalance compensation for optimal power quality in islanded microgrids, *IEEE Trans. Energy Conversion*, vol.29, no.4, pp.802-815, 2014.

[19] J. Guerrero, P. Loh, M. Chandorkar and T. Lee, Advanced control architectures for intelligent MicroGrids – Part I: Decentralized and hierarchical control, *IEEE Trans. Ind. Electron.*, vol.60, no.4, pp.1254-1262, 2013.

[20] M. Savaghebi, A. Jalilian, J. C. Vasquez and J. M. Guerrero, Autonomous voltage unbalance compensation in an islanded droop-controlled microgrid, *IEEE Trans. Ind. Electron.*, vol.60, no.4, pp.1390-1402, 2013.

[21] M. Savaghebi, A. Jalilian, J. C. Vasquez and J. M. Guerrero, Secondary control scheme for voltage unbalance compensation in an islanded droop-controlled microgrid, *IEEE Trans. Smart Grid*, vol.3, no.2, pp.797-807, 2012.

[22] C. Yuen, A. Oudalov and A. Timbus, The provision of frequency control reserves from multiple microgrids, *IEEE Trans. Ind. Electron.*, vol.58, no.1, pp.173-183, 2011.

[23] Y. Zhang and H. Ma, Theoretical and experimental investigation of networked control for parallel operation of inverters, *IEEE Trans. Ind. Electron.*, vol.59, no.4, pp.1961-1970, 2012.

[24] J. M. Guerrero, J. Matas, L. G. de Vicuna, M. Castilla and J. Miret, Decentralized control for parallel operation of distributed generation inverters using resistive output impedance, *IEEE Trans. Ind. Electron.*, vol.54, no.2, pp.994-1004, 2007.

[25] E. Barklund, N. Pogaku, M. Prodanović, C. H. Aramburo and T. C. Green, Energy management in autonomous microgrid using stability-constrained droop control of inverters, *IEEE Trans. Power Electron*, vol.23, no.5, pp.2346-2352, 2008.

[26] Q. Liu, Y. Tao, X. Liu, Y. Deng and X. He, Voltage unbalance and harmonics compensation for islanded microgrid inverters, *IET Power Electron*, vol.7, no.5, pp.1055-1063, 2014.

[27] A. Ovalle, G. Ramos, S. Bacha and A. Hably, Decentralized control of voltage source converters in microgrids based on the application of instantaneous power theory, *IEEE Trans. Ind. Electron.*, vol.62, no.2, 2015.

[28] J. Vasquez, J. M. Guerrero, M. Savaghebi, J. Eloy-Garcia and R. Teodorescu, Modeling analysis and design of stationary reference frame droop controlled parallel three-phase voltage source inverters, *IEEE Trans. Ind. Electron.*, vol.60, no.4, pp.1271-1280, 2013.

[29] J. He and Y. W. Li, An enhanced microgrid load demand sharing strategy, *IEEE Trans. Power Electron*, vol.27, no.9, pp.3984-3995, 2012.